Surface Analysis of Poly(vinyl alcohol-*co*-*N*-vinyl-2-pyrrolidone) Copolymers by X-ray Photoelectron Spectroscopy

Donald R. Miller† and Nikolaos A. Peppas*

School of Chemical Engineering, Purdue University, West Lafayette, Indiana 47907.
Received July 29, 1986

ABSTRACT: Random copolymers of poly(vinyl acetate-*co*-*N*-vinyl-2-pyrrolidone), P(VAc-*co*-NVP), were synthesized with vinyl acetate mole fractions f_1 = 0.0, 0.2, 0.4, 0.6, 0.8, and 1.0. The copolymers were converted to poly(vinyl alcohol-*co*-*N*-vinyl-2-pyrrolidone), P(VA-*co*-NVP), by alkaline methanolysis. The degree of conversion of VAc units to VA was greater than 97 mol %. Hydrogels of P(VA-*co*-NVP) were produced by cross-linking of an aqueous solution of P(VA-*co*-NVP) with γ-irradiation at 35 °C. Bulk composition analysis was evaluated by IR, NMR, and elemental analysis. The surface composition was evaluated by X-ray photoelectron spectroscopy (XPS) of freeze-dried samples of the hydrogels. Quantitative XPS analysis demonstrated a surface enrichment of the VA units in copolymers with VA molar fraction of $F_1 < 0.34$. This perturbation from the most probable distribution near the hydrogel surface resulted from the presence of macromolecules with chain lengths significantly shorter than the average chain length. The effect of freeze drying on XPS analysis was investigated by surface esterification of the VA units of the hydrogels. The XPS penetration depth in freeze-dried materials, the sputtering of polymer surfaces, and the effect of cross-linking on surface compositions were also investigated.

Introduction

In the development of biocompatible polymers for artificial organs there are many unanswered questions concerning the fundamental understanding of blood/polymer interactions. One possible reason for the belated advancement in this area is the lack, until recently, of sophisticated techniques to probe the surface of materials. Insufficient knowledge of the blood coagulation mechanism is another important factor.[1]

Major recent developments in the fields of surface analysis and blood clotting have led to new directions in biomaterials research. Unfortunately, the work to date has not made full use of surface analysis of blood/polymer interfaces at the molecular level. The relationship between blood protein adsorption and the surface composition of a polymer (not bulk composition as several researchers have used) has not been adequately studied. In the past few years, several good research contributions have appeared that describe surface analysis of various polymers for biomedical applications (e.g., Avcothane, Biomer, Polyacrylamide/Silastic, etc.).[1-3] In these studies, the effort has been more toward evaluation of the biocompatibility of these materials rather than fundamental investigation of blood protein/polymer interactions.

The studies conducted in this work were directed toward a through understanding of the hydrogel/water interface and the factors affecting the surface structure of the swollen polymeric network (hydrogel). These studies were performed with a model copolymer, poly(vinyl alcohol-*co*-*N*-vinyl-2-pyrrolidone), henceforth designated as P(VA-*co*-NVP).

Experimental Methods

Preparation of Polymers. The copolymers and homopolymers synthesized were produced by reaction of *N*-vinyl-2-pyrrolidone (NVP) and vinyl acetate (VAc) (Aldrich Chemical Co., Milwaukee, WI) at 35 °C using γ-rays as the initiator. Methanolysis and cross-linking were employed to produce highly swollen networks of the homo- and copolymers, as discussed in a previous publication.[4]

Methanolysis of the VAc units in the copolymer was achieved by reacting a 10 wt % polymer solution with an aqueous NaOH solution. The reaction was carried out at ambient temperature for 36 h and terminated by addition of a 1.0 M aqueous HCl solution. Methanolysis byproducts (sodium acetate, methyl acetate, NaCl) were removed by dialysis.

Networks of the co- and homopolymers were synthesized by irradiating 5 wt % aqueous solutions under a nitrogen atmosphere at 35 °C in glass Petri dishes. Swollen networks were produced by soaking the sample in deionized water at 35 °C for several days. The volume swelling ratio was evaluated from the buoyancy of the network in cyclohexane before (swollen state) and after drying.

Bulk Polymer Characterization. Nuclear magnetic resonance spectroscopy and infrared spectroscopy were used for quantitative analysis of the polymer composition using a FT80 NMR spectrometer system (Varian, Palo Alto, CA). The P(VAc-*co*-NVP) copolymers were studied in deuteriated chloroform (Aldrich Chemical Co., Milwaukee, WI.); the P(VA-*co*-NVP) copolymers were evaluated in deuterium oxide (Baker Chemical Co., Phillipsburg, NJ). Infrared spectroscopy (IR) was accomplished with an IR-33 (Beckman Instruments Inc., Irvine, CA). The polymer samples were studied by forming a KBr pellet. Elemental analysis of the polymer samples was also performed for hydrogen, carbon, and nitrogen.[4] Nitrogen analysis was based on the modified Kjeldahl method and was done immediately following the carbon/hydrogen analysis.[5] Samples were initially dried before analysis and analyzed under a dry nitrogen atmosphere.

X-ray Photoelectron Spectroscopy. The instrument employed for X-ray photoelectron spectroscopy (XPS) was a Physical Electronics (PHI) Model 550 ESCA/SAM system (Norwalk, CT). The X-ray source was a nonmonochromatic Mg anode operated between 150 and 400 W of emissive power. An electron gun was utilized for charge neutralization of the nonconducting samples at 0.0-V bias and 0.15-mA emission current. The operating pressure of the instrument was (2–6) × 10^{-8} Torr.

For sputtering studies, the ion gun used was situated normally to the sample surface. The ion current employed was approximately 2.9 μA with a rastering area of 0.8 × 0.8 cm.

The surface esterification of the VA units in the copolymers was achieved by using a modified Pennings and Bosman[6] procedure. The labeling solution contained 5 mL of heptafluorobutyric acid chloride (HFBC) (Fluka Chemical Co., Hauppauge, NY), 2.7 mL of pyridine, and 92.3 mL of *n*-hexane. A swollen polymer sample approximately 1.0 × 1.0 cm was placed in 15 mL of the labeling solution and reacted for 30 min at ambient temperature without stirring. The reacted samples were then placed in 5 vol % HCl solution (of 36 vol % HCl) for 2 h to convert any remaining pyridine to pyridinium chloride, which was removed by soaking the samples in deionized water for 2 days with repeated solution changes.

The swollen samples for XPS studies were handled by placing them on a cold probe that contained liquid nitrogen. Each sample was allowed to equilibrate for several minutes, placed in the prechamber for 10 min, and inserted into the X-ray beam in the

†Present address: Lederle Laboratories, Pearl River, NY 10965.

0024-9297/87/2220-1257$01.50/0

Table I
C_{1s} XPS Peak Shape Alterations as a Function of X-ray Dose for a P(VA-*co*-NVP) Copolymer Sample with $F_1 = 0.34$

X-ray dose, min	peak position, eV	fwhm, eV
55	286.2	2.34
115	286.2	2.31
125	285.0	2.34

main chamber. The samples were analyzed for only several minutes due to the drastic rise in instrument pressure.

Results and Discussion

Instrument Resolution and Calibration. The Au $4f_{7/2}$ photopeak with a literature value[7] of 83.8 ± 0.2 eV was employed as a standard to evaluate the resolution and binding energy scale of the XPS instrument. The value obtained was 83.6 eV without charge correction.

Charging Effects. The polymer samples studied were insulating materials that required charge compensation for the electrons removed by photoemission. The electron flood gun was operated at essentially zero potential with respect to the sample probe.

The broad XPS peaks for polymer samples have been attributed to conducting paths produced in regions of the sample due to X-ray damage[7] which tends to produce differential charging of the sample surface. This type of differential charging was rather small in our studies and invariant to the charge compensation due to the large XPS sampling area. If the sample has macrodifferential charging, variation of the charge compensation could produce fwhm shifts of the photopeaks. For example, fwhm of a P(VA-*co*-NVP) copolymer with $F_1 = 0.34$ mole fraction of VA units was not affected as the charge compensation was varied. Thus, it was concluded that the polymer samples studied here did not show macrodifferential charging.

X-ray Effects on Polymers. To minimize X-ray effects and discoloration, the lowest possible acquisition periods were employed. The XPS spectra of P(VA-*co*-VAc) and PNVP were compared before and after prolonged exposure to the X-ray source. For the P(VA-*co*-VAc) samples, the X-rays altered the peak shapes of the carbon and oxygen photopeaks respectively 285 and 530 eV. The P(VA-*co*-VAc) samples appeared to be affected by X-rays to a greater degree than PNVP samples. Measurements of the C_{1s} photopeak area and fwhm of a copolymer with $F_1 = 0.34$ were taken with different X-ray exposure periods. The peak results are given in Table I.

The peak shapes, indicated by the fwhm values in Table I, were invariant to X-ray dose, as were the peak areas. The sample color alteration and the survey scan results indicated that the polymers were damaged by the X-rays but to a degree that was sufficiently low that it did not perturb peak shapes. The binding energy shift in the 125-min X-ray dose sample in Table I was due to a change in the electron flood gun current.

Polymer Standard. As an evaluation of polymer quantitative analysis and peak shape, a film of Teflon was used as a standard. The survey analysis indicated only F and C on the surface; these were quantitatively studied by using area ratios giving an atomic concentration ratio of $N_F/N_C = 2.0$. Correlation of the C_{1s} data provided a peak shape that was 91.4% Gaussian in character when analyzed with a linear sum function.

XPS Instrument Constants. Instrument factors were obtained by XPS analysis of standards such as pure homopolymers of PVA and PNVP. The XPS intensity ratios were related to the material composition by utilizing the copolymer repeating unit structure to derive eq 1 and 2 in conjunction with the homogeneous XPS equations[8]

$$I_C/I_O = I_{CO} = K_{CO}(6 - 4F_1) \quad (1)$$

$$I_N/I_O = I_{NO} = K_{NO}(1 - F_1) \quad (2)$$

where

$$K_{ij} = \frac{\lambda_i \sigma_i}{\lambda_j \sigma_j} \frac{D_i}{D_j}$$

The values of the parameters of K_{ij} were taken[9] as λ_C = 29.0 Å, $\sigma_C = 1.00$, λ_N = 27.3 Å, $\sigma_N = 1.77$, λ_O = 25.0 Å, and $\sigma_O = 2.85$. Substitution of the relevant parameters into K_{ij} gave

$$K_{CO} = 0.407 D_C/D_O \quad (3)$$

$$K_{NO} = 0.678 D_N/D_O \quad (4)$$

The D_i terms in eq 3 and 4 are instrument factors that account for the varying efficiency of the β spectrometer at different β-particle kinetic energies and the detector efficiency.

Table II
Determination of XPS Equipment Constants

sample	I_{CO}	I_{NO}	N_{CO}	N_{NO}	K_{CO}	K_{NO}
PVAc	0.68		2		0.34	
PVA	0.76		2		0.38	
PNVP	2.18	0.54	6	1	0.36	0.54
PNVP	2.21	0.60	6	1	0.37	0.60
PNVP	2.25	0.53	6	1	0.37	0.53

Table II presents the results of XPS analysis of PVA, PNVP, and PVAc homopolymers. The PVAc sample was solvent-cast onto a glass slide; all other samples reported in Table II were cross-linked (2.28 Mrad), freeze-dried membranes. The values of K_{CO} and K_{NO} were obtained by averaging the above values as $K_{CO} = 0.37 \pm 0.01$ and $K_{NO} = 0.5 \pm 0.10$. The limits on K_{CO} and K_{NO} are the 95% confidence limits for 3 and 2 degrees of freedom, respectively. The XPS intensity ratios are given by eq 1, 2, and 5

$$I_{CN} = K_{CN} \frac{(6 - 4F_1^s)}{(1 - F_1^s)} \quad (5)$$

where I_{ij} is the XPS intensity ratio of species i to j and F_1^s is the surface region mole fraction of VA units. Solving eq 2 for F_1^s and substituting this expression into eq 1 result in eq 6.

$$I_{NO} = \tfrac{1}{4}(K_{NO}/K_{CO}) I_{CO} - \tfrac{1}{2} K_{NO} \quad (6)$$

The plot of I_{NO} and I_{CN} vs. I_{CO} XPS data for the various copolymers and homopolymers studied is presented in Figure 1. The plot of I_{NO} vs. I_{CO} produced a straight line with a slope of 0.39 ± 0.02, an intercept of −0.29 ± 0.03, and $r^2 = 0.983$. From eq 6, the instrument constants were $K_{NO} = 0.584$ and $K_{CO} = 0.374$. These values compare well with the results discussed above from the homopolymers and are within the error limits given previously. The good correlation of the XPS data to eq 6 was a verification of the copolymer structure.

XPS Penetration Depth in Hydrogels. The classic XPS theory is normally applied to materials that are dense and homogeneous laterally and axially.[8,10] The assumption of axial and lateral homogeneity can be tested by several techniques, two of which are angle-resolved XPS and scanning Auger spectroscopy.[8,11] The polymer samples studied here could be readily analyzed by the standard differential homogeneous XPS analysis using eq 7.

$$dI = \frac{F_0 \sigma N D}{\sin \theta} e^{-x/(\lambda \sin \theta)}\, dx \quad (7)$$

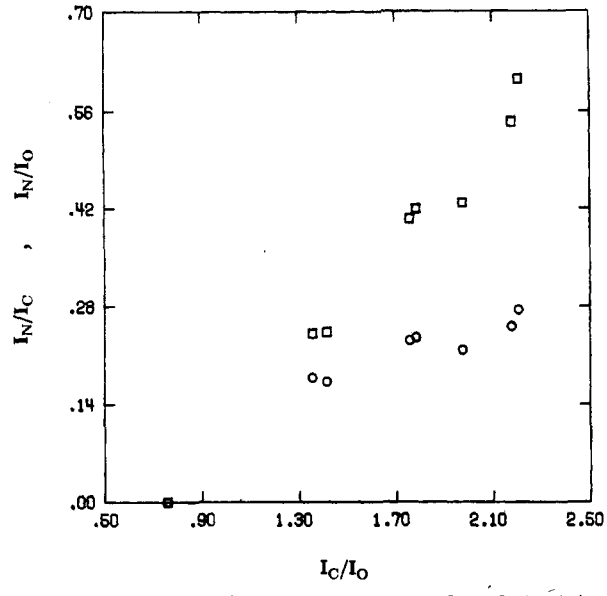

Figure 1. X-ray photoelectron nitrogen-to-carbon, I_N/I_C (□) and nitrogen-to-oxygen ratios, I_N/I_O (○) as functions of the carbon-to-oxygen ratio, I_c/I_o, for freeze-dried PVA, PNVP, and P(VA-*co*-NVP) samples.

When eq 7 is integrated from zero depth to infinity, eq 8 is obtained, which relates the intensity of a elemental peak to factors that can either be measured or obtained as lumped parameters.

$$I_\infty = F_0\sigma\lambda DN \tag{8}$$

All the hydrogel samples used here were freeze-dried before surface analysis. Since photoelectrons are attenuated only by the polymer, the voids act as transport paths for the electrons without attenuation (reflection of electrons and photons at polymer/void interfaces is assumed negligible).

A differential mass balance in the sampling region was employed by assuming randomly distributed voids, i.e., values of the polymer volume fraction, υ_{2s}, that were position-invariant.

$$A\ dx_{pv}\ \upsilon_{2s} = A\ dx_p \tag{9}$$

Here x_{pv} is the total length of a polymer/void element, A is the area of sample zone, and x_p is the length of equivalent solid polymer element. Thus, the freeze-dried samples were treated as equivalent solid polymers of reduced thickness. The depth values used in eq 7 were replaced by x_p and dx_p and eq 10 was used for the analysis.

$$dI = \frac{F_0\sigma ND\upsilon_{2s}}{\sin\theta} e^{-x\upsilon_{2s}/(\lambda\sin\theta)}\,dx \tag{10}$$

Equation 10 results in eq 8 after infinite depth integration due to the cancellation of the $\upsilon_{2s}/\sin\theta$ terms. The obvious effect of the void fraction is to modify the penetration depth of the experiment. This can be seen from integration of eq 10 from zero to a depth of ζ into the system.

$$I = I_\infty\left(1 - \exp\left(\frac{-\zeta\upsilon c_{2s}}{\lambda\sin\theta}\right)\right) \tag{11}$$

Therefore, the cumulative fractional intensity, f, obtained from a depth ζ is given by

$$f = \frac{I}{I_\infty} = 1 - \exp\left(\frac{-\zeta\upsilon_{2s}}{\lambda\sin\theta}\right) \tag{12}$$

The fractional intensity, f, from eq 12 as a function of sample depth is presented in Figure 2 for carbon, oxygen, and nitrogen photoelectrons, using $\theta = 50°$, $\upsilon_{2s} = 1.0$, and λ values previously discussed.

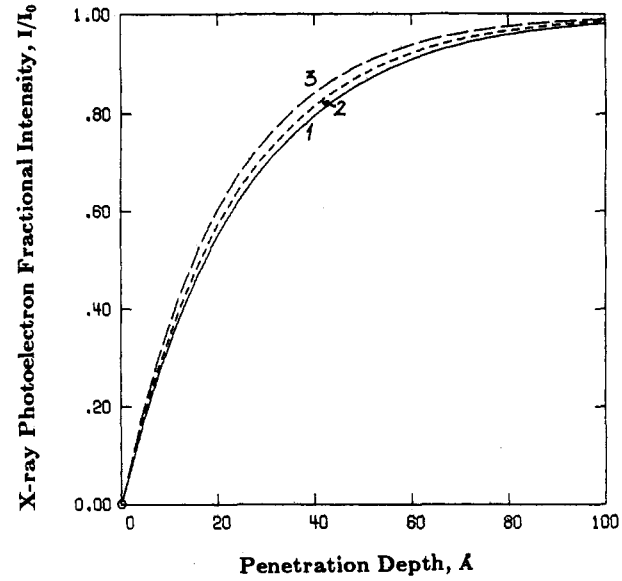

Figure 2. X-ray photoelectron fractional intensity of C_{1s} (curve 1), O_{1s} (curve 2), and N_{1s} (curve 3) as a function of sampling depth calculated for a polymer with density of 1.2 g/cm³.

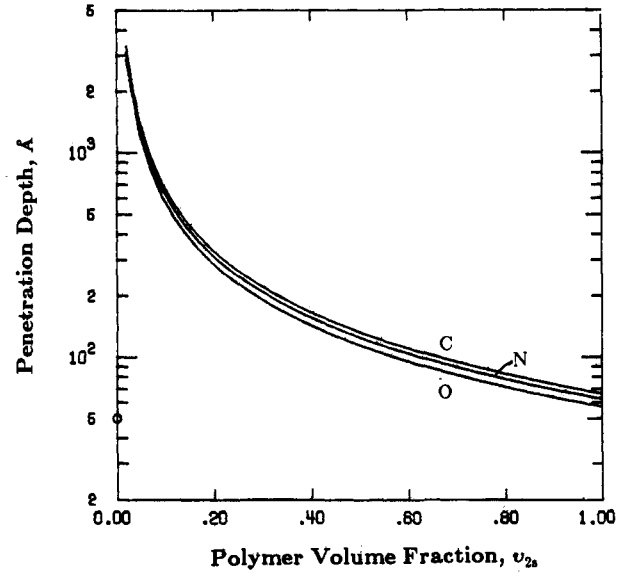

Figure 3. X-ray photoelectron penetration depth as a function of equilibrium polymer volume fraction in the freeze-dried sample.

The effect of voids on penetration depth is shown in Figure 3, using eq 12 and the same θ and λ values as in Figure 2. The large XPS penetration depths in highly perturbed freeze-dried membranes required comparison to the length scale of a single polymer chain. For polymer samples of $\bar{M}_n$ = 40 000 (as determined by GPC) and typical swelling ratios, the end-to-end distance was approximately 300 Å for PNVP and 400 Å for PVA. Comparison of these values with the results of Figure 3 suggested an XPS sampling region of between 5 and 10 polymer chain lengths. Since the polymers analyzed by XPS were cross-linked, the chain lengths given above represented upper limits for polymer length scale. It is interesting to note that the chain length increases as $Q^{1/3}$, where Q is the volume swelling ratio of the polymer (= $1/\nu_2$), while the XPS penetration depth increases as Q, according to eq 12, with all other terms held constant. Thus, the number of polymer chains sampled increases approximately as $Q^{2/3}$.

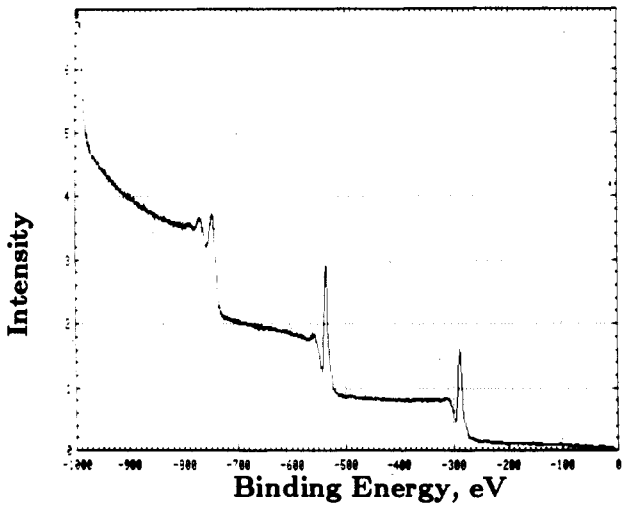

Figure 4. X-ray photoelectron C_{1s} spectrum of P(VA-*co*-VAc) copolymer.

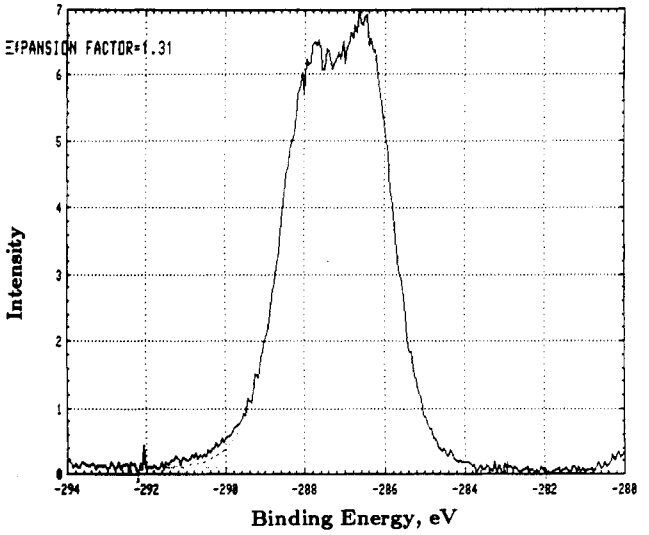

Figure 5. X-ray photoelectron C_{1s} spectrum of PVA.

PVA and PNVP XPS Analysis. The PVA samples studied in this work were produced by alkaline methanolysis of PVAc to a degree greater than 97% (negligible effect of residual acetate content). The survey scan of a partially converted PVAc sample is presented in Figure 4.

With peak height analysis, the mole fraction of VA was estimated by peak height measurements of the P(VA-*co*-VAc) spectra. The height of the C_{1s} shoulder at 290 eV was measured (carbonyl of acetate repeating unit) and compared to the height of the main carbon peak. This produced a VA composition of 81 mol %, whereas with the oxygen peak heights the composition was 91 mol % VA units. Bulk analysis of this P(VA-*co*-VAc) copolymer with NMR produced a VA content of 36 mol %. Comparison of the bulk and surface compositions indicated that the copolymer was enriched in VA units in the surface region due to the hydrophilic "template" used to form the hydrogel.

The C and O photopeaks of the XPS spectra of a highly methanolyzed PVAc sample, i.e., PVA, are presented in Figures 5 and 6, respectively. The peak shapes were considerably altered from the partially methanolyzed sample, with the carbon peak indicating only two oxidation states. This result is consistent with a VA structure that is composed of two carbon states. The peak data for a PVA sample are given in Table III.

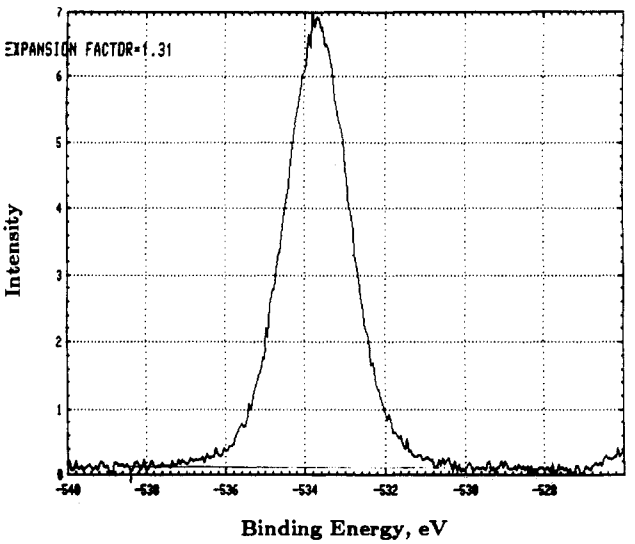

Figure 6. X-ray photoelectron O_{1s} spectrum of PVA.

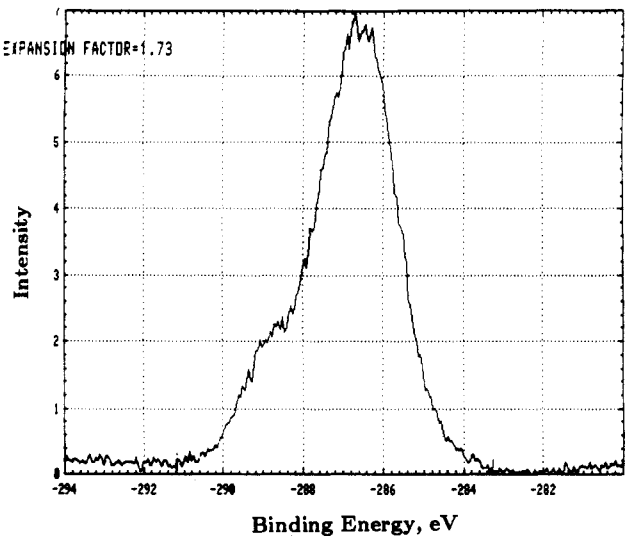

Figure 7. X-ray photoelectron C_{1s} spectrum of PNVP.

Table III
Analysis of XPS Peak Data for PVA

peak	position, eV	fwhm, eV
C_{1s}	286.6	2.9
O_{1s}	533.7	1.8
O_{KLL}	745.2	

Table IV
Analysis of XPS Peak Data for PNVP

peak	position, eV	fwhm, eV
C_{1s}	286.6	2.32
N_{1s}	400.8	1.71
O_{1s}	532.1	2.00
O_{KLL}	744.3	

Analysis of the surface of the PNVP homopolymer was different from that of the PVA sample not only due to structural modifications but also due to the presence of the element nitrogen. The C_{1s}, N_{1s}, and O_{1s} photopeaks are shown in Figures 7–9, respectively. The XPS data for this sample are given in Table IV.

Quantitative Analysis of P(VA-*co*-NVP). The polymer hydrogels formed in this study essentially precipitated onto the bottom of a Petri dish during irradiation. This process resulted in hydrogels that had two primary faces which were formed in different environments; one side was exposed to the glass/polymer interface while the

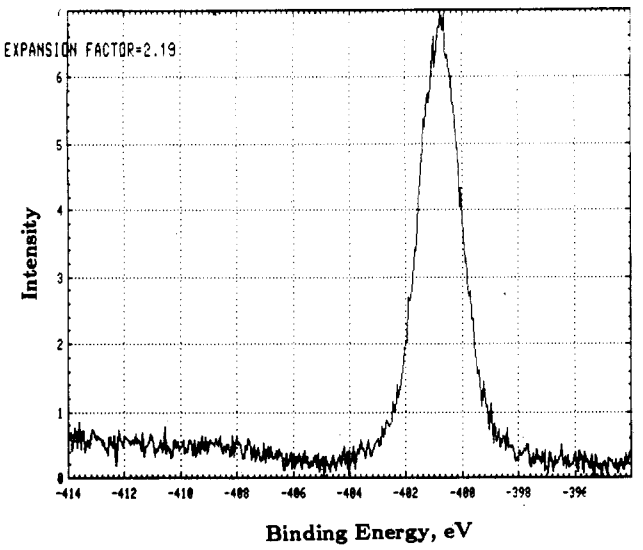

Figure 8. X-ray photoelectron N_{1s} spectrum of PNVP.

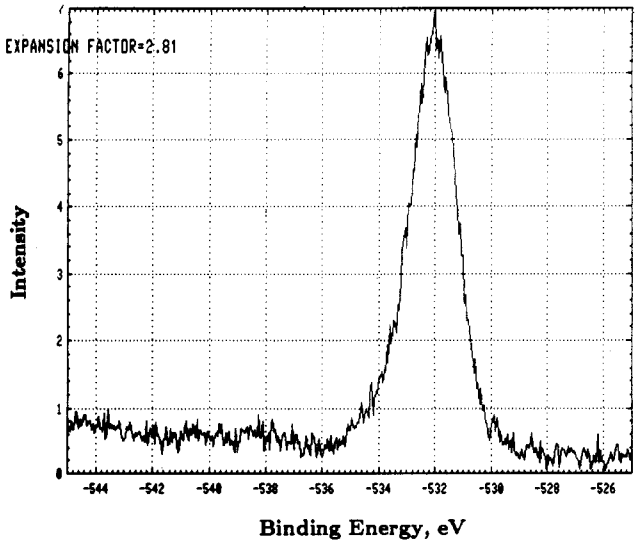

Figure 9. X-ray photoelectron O_{1s} spectrum of PNVP.

Table V
Analysis of XPS Peak Data for Freeze-Dried P(VA-*co*-NVP) Copolymer Samples Formed against a Glass Surface by γ-Irradiation with 2.28 Mrad

F_1	I_{CO}	I_{NO}	F^s_{1CO}	F^s_{1NO}
1.00	0.756		0.99 ± 0.03	
0.59	1.385	0.242	0.57 ± 0.05	0.57 ± 0.11
0.34	1.755	0.405	0.32 ± 0.06	0.28 ± 0.18
0.17	1.781	0.419	0.30 ± 0.06	0.25 ± 0.19
0.13	1.973	0.428	0.17 ± 0.07	0.23 ± 0.19
0.00	2.191	0.575	0.02 ± 0.08	0.00 ± 0.26

other side was formed at the sol fraction interface (solvent and un-cross-linked polymer chains). Table V contains XPS results for cross-linked, freeze-dried polymer hydrogels formed against the glass interface. All the hydrogels in Table V were cross-linked with a γ-ray dose of 2.28 Mrad. The intensity of their photopeaks was defined with the Shirley[12] method.

The F_1^s terms in Table V contain an added subscript of either CO or NO that specifies the intensity ratio that was employed for the calculation. The two values of F_1^s for each sample in Table V agreed well within the error limits. The surface composition of the hydrogels was in agreement with the bulk values except for low values of VA in the copolymer. The hydrogels with $F_1 = 0.17$ and 0.13 contained additional VA units when compared to the

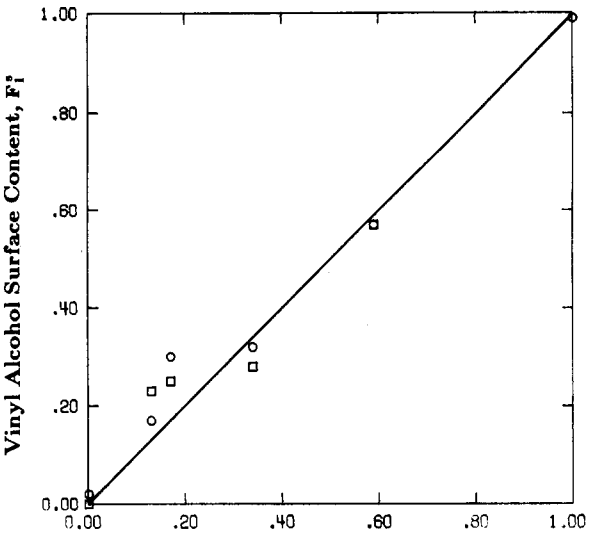

Figure 10. Vinyl alcohol surface content, F_1^s, of P(VA-*co*-NVP) copolymer as a function of the vinyl alcohol bulk composition, F_1, from I_{CO} (○) and I_{NO} (□) values.

Table VI
Statistical Analysis of Data for Bulk and Surface Compositions

VA mol fract in copolym, F_1	t_{calcd}	ν	t_{tab} 90%	t_{tab} 95%
0.13	2.31	3	1.638	2.353
0.17	2.96	3	1.638	2.353
0.34	1.40	3	1.638	2.353
0.59	∞	3	1.638	2.353

bulk values. This can be seen in Figure 10, where F_1^s is plotted vs. F_1.

The significance of the difference between the mean value of F_1^s obtained by XPS and the bulk copolymer composition value F_1 was evaluated by the t test. The quantity t is defined as the difference of the two means divided by the standard deviation.

$$t = \frac{\bar{X}_1 - \bar{X}_2}{[(S_1^2/N_1) + (S_2^2/N_2)]^{1/2}} \tag{13}$$

Here $\bar{X}_i$ represents the mean value for data set i and S_i and N_i are the standard deviation and number of data points for data set i. The number of degrees of freedom, ν, for the t test is defined as $\nu = N_1 + N_2 - 2$. The results of the significance test are presented in Table VI. The terms t_{tab} and t_{calcd} refer to tabulated t values and calculated t values, respectively. The low-VA-containing samples ($F_1 = 0.13$ and 0.17) conclusively pass the t test at the 90% level (probability is 90% that the means of the bulk and surface composition values are significantly different). The sample with $F_1 = 0.34$ did not pass the t test and satisfied the null hypothesis at the 90 and 95% levels. In the analysis of the sample with $F_1 = 0.59$, the bulk and surface data had variances that were essentially zero, resulting in any difference being significant (this is just a artifact due to the low number of samples). Thus, the surface of the copolymers was enriched in VA units at low values of F_1 and identical with the bulk values when F_1 reached 0.34.

The enrichment of the copolymer surface can be qualitatively explained by thermodynamic arguments. During cross-linking at the glass/polymer solution interface, the low free component of a binary mixture is preferentially adsorbed to minimize the interfacial free energy. A

qualitative measure of the tendency of a species to cover a surface is the work of adhesion, W_{adh}, i.e., the reversible work required to separate the two surfaces. For the P(VA-*co*-NVP) samples, the surface tensions[13] are γ_1 = 58.7 (glass), γ_2 = 37.0 (PVA), γ_3 = 53.6 (PNVP), and γ_4 = 72.8 dyn/cm (water). If NVP is excluded from the analysis, the work of adhesion is

$$W_{adh} = \gamma_{24} + \gamma_{14} - \gamma_{12} \quad (14)$$

where the surface tension between two components is approximately given by

$$\gamma_{ij} = (\gamma_i^{1/2} - \gamma_j^{1/2})^2 \quad (15)$$

Application of eq 14 and 15 gives the W_{adh} of a VA unit onto glass of 0.00427 J/m^2. The work of adhesion for the NVP unit on glass, excluding species VA, is given by eq 16. When the same analysis as with PVA is employed,

$$W_{adh} = \gamma_{34} + \gamma_{14} - \gamma_{13} \quad (16)$$

the work of adhesion for NVP is W_{adh} = 0.00211 J/m^2. Thus, the VA unit is thermodynamically favored to adhere to the glass surface. The surface is not completely covered by VA units due to its attachment to a random copolymer chain and competitive adsorption. To accurately predict the surface composition, the sequence length of the low-energy species (VA) and the quantity of this species must be considered in addition to the thermodynamic factors.

The above discussion addressed the cause of the enrichment in VA units at the network interface but not the likelihood of such an occurrence. For random copolymers, the ratio of the monomers incorporated in the final copolymer is predicted by the most probable distribution of eq 17

$$\phi(N) = P_i^M P_2^{N-M} \frac{N!}{(N-M)!M!} \quad (17)$$

where $\phi(N)$ is the number fraction of a chain with N total units containing M units of type 1 (VA units in this case) and P_1 and P_2 are the probabilities of incorporating species 1 and 2, given by

$$P_1 = \frac{f_1 r_1}{r_2 + f_1(r_1 - r_2)}$$

$$P_2 = \frac{(1 - f_1) r_2}{r_2 + f_1(r_1 - r_2)}$$

Also f_1 is the mole fraction of species 1 in the comonomer mixture and r_1 and r_2 are the reactivity ratios, measured previously.[4] Thus

$$\phi(N) = (f_1 r_1)^M (r_2(1 - f_1))^{N-M} (r_2 + f_1(r_1 - r_2))^{-N} \frac{N!}{(N-M)!M!} \quad (18)$$

and

$$W(N) = \left[1 + \frac{1}{\phi(N)} \frac{M_1}{M_2} \right]^{-1}$$

where $W(N)$ is the weight fraction of 1 in a chain of N units and M_i is the repeating unit molecular weight. If Z g of copolymer were placed in water to form a network, then the maximum depth, d, for the VA-enriched chains at the network interface is given by

$$d = \int_1^{N'} \frac{Z w(N) W(N)}{A v_2 \rho_p} \, dN = \frac{Z}{A v_2 \rho_p} \int_1^{N'} w(N) W(N) \, dN \quad (19)$$

Table VII
Effect of Cross-Linking on XPS Analysis of Freeze-Dried P(VA-*co*-NVP) Copolymer Samples

VA mol fract in bulk copolym, F_1	irradiation dose, Mrad	fwhm, eV		
		C_{1s}	O_{1s}	N_{1s}
0.00	0.00	2.2	2.2	1.8
0.00	2.28	2.4	2.4	1.9
0.00	10.00	2.6	2.5	1.7
0.59	2.28	2.4	1.9	1.7
1.00	0.00	2.4	1.9	
1.00	2.28	2.9	1.8	
1.00	10.00	3.16	2.7	

where $w(N)$ is the copolymer weight fraction with chains of length N and A, v_2, and ρ_p are the network axial surface area, the volume swelling ratio, and the copolymer density, respectively.

The proof of plausibility of the VA enrichment at the network interface lies on the determination of the enriched VA copolymer segment depth from eq 19, which must be at least comparable to the XPS penetration depth. Indeed, using reasonable values for the parameters appearing in eq 18 and 19, we concluded that there is a sufficient depth d to cause surface enrichment (this enrichment is due primarily to smaller chains where the probability for enrichment is greatest).

Effect of Cross-Linking. The effect of cross-linking was evaluated for several P(VA-*co*-NVP) samples (Table VII). The solvent-cast samples indicated that cross-linking of the polymers produced some broadening of the carbon and oxygen peaks. This was most pronounced for the PVA samples. The hydrogen bonding of the VA units should contribute to the lower fwhm of PVA in the solvent-cast samples compared to the freeze-dried, cross-linked samples.

The oxygen peak of PVA was drastically broadened with high degrees of cross-linking, since during irradiation oxygen diffuses into the system. The broadening of the XPS photopeaks by cross-linking did not affect quantitative analysis, but the inclusion of extra oxygen into the polymer network by diffusion had adverse effects. The samples of primary study in this work were the low-cross-linked samples, prepared by irradiation with 2.28 Mrad. The quantitative results of XPS analysis of the low-cross-linked hydrogels produced consistent instrument factors. The peak shapes of the 2.28-Mrad PVA hydrogels were in good agreement with the repeating unit structure.

XPS Analysis of Swollen Polymers. In an effort to examine modifications due to freeze-drying effects, a polymer sample was chosen for XPS analysis in both the freeze-dried (fd) and the swollen state (sw); the comparison of results obtained in both states allows the examination of possible polymer surface alterations due to a diluent phase change.

The effect of a diluent on XPS studies must be first evaluated to enhance data analysis. Examination of the nitrogen-to-carbon intensity ratio results in

$$\frac{I_N}{I_O} = \frac{\sigma_N \lambda_N D_N}{\sigma_O \lambda_O D_O} \left\{ 1 + \frac{\rho_w}{\rho_p}(Q - 1) \frac{[F_1 M_{r1} + (1 - F_1) M_{r2}]}{M_w} \right\}^{-1} F_2 \quad (20)$$

An interesting comparison is obtained if the ratio I_N/I_O for the freeze-dried state is divided by the same ratio for the swollen state

$$\frac{(I_N/I_O)_{fd}}{(I_N/I_O)_{sw}} = F_1\left\{\frac{1}{F_1} + \frac{\rho_w}{\rho_p}(Q-1)\frac{[M_{r1} + [(1/F_1) - 1]M_{r2}]}{M_w}\right\} \quad (21)$$

Here M is the total moles of polymer chains/unit volume ($=\rho_p/M_n$), Q is the volume swelling ratio of polymer ($= 1/v_2$), F_i is the mole fraction of species i units in the copolymer, n_i is the number of repeating units of species i contained in a polymer chain, ρ_i is the mass density of species i, M_{ri} is the molecular weight of repeating unit of species i, γ_i is the full width of photopeak at half of peak maximum of peak i, M_p is the total moles of polymer, N_{ri} is the total number of species i repeating units, N is Avogadro's number, N_{pc} is the total number of polymer chains, and N_i^j is the atomic density of element i in species j. Henceforth, the vinyl alcohol (VA) repeating units will be designated by the subscript 1 and the *N*-vinyl-2-pyrrolidone (NVP) repeating units by 2.

The term on the right in eq 21 is essentially the reciprocal of an attenuation factor for the presence of water in the hydrogel. This analysis of course assumes no interfacial water is present on the surface of the material.

When $Q = 1$ (only polymer present), the freeze-dried and swollen states of course had the same intensity ratios. The presence of the diluent in the XPS sample affected the surface analysis in several ways: (i) the elemental photopeak intensities of the sample were altered and (ii) the photopeak shape was modified since water contained elements common with the sample. The results of the XPS study on the swollen ($Q = 24$) and freeze-dried states of the P(VA-*co*-NVP) copolymer sample with $F_1 = 0.59$ are presented in Table VIII.

From the above theoretical analysis, the I_i/I_O intensity ratio for species i should be considerably lower in the swollen state than in the freeze-dried state. The carbon-to-nitrogen ratio should be the same in either state. Analysis of the data presented in Table VIII results in several important observations and conclusions:

(i) The carbon-to-oxygen ratio is higher in the swollen state than in the freeze-dried state.

(ii) The nitrogen-to-oxygen ratio is qualitatively in agreement with eq 21 and is lower in the swollen state.

(iii) The carbon-to-nitrogen ratio is higher in the swollen state than in the freeze-dried state.

(iv) The swollen-state intensity ratios are too high for such a highly hydrated hydrogel.

(v) Only the oxygen peak's full width at half maximum changed from the swollen to freeze-dried states.

Conclusions (i) and (iii) above indicated that carbon contamination occurred in the swollen samples. This is not an unexpected problem and has been seen by other researchers.[14] The carbon deposition is primarily due to the cryogenic temperature of the sample surface. The contamination was sufficient to overcome the increase in oxygen concentration in the swollen state, which resulted in a higher I_C/I_O for the swollen state.

The nitrogen-to-oxygen ratio followed the theoretical analysis and was lower in the swollen state, suggesting that nitrogen contamination of the swollen sample was negligible. Carbon contamination for the swollen sample affected the nitrogen-to-oxygen ratio in addition to the effect of water. The effect of a contamination layer of thickness δ modifies the term I_N/I_O by the factor of

$$\{I_N/I_O\}_{cont} = \{I_N/I_O\} \exp[-\delta(1/\lambda_N - 1/\lambda_O)/\sin\theta] \quad (22)$$

Conclusion (iv) indicated that sublimation must have occurred on the polymer surface in the spectrophotometer. The XPS studies of Hirokawa and Danzaki[15] on inorganic gels demonstrated that the samples lost their coordination water at −50 °C after 1 h in the spectrometer.

The photopeak full widths at half maximum of the carbon and nitrogen were essentially unchanged in either state, indicating no extra oxidation states of these elements. The carbon spectral envelope was very broad, which accounted for the lack of broadening even though carbon contamination was present. With the oxygen peak, narrowing of the envelope further substantiated the belief that extra oxygen was present (from water) in sufficient quantities to alter peak shapes.

Sputtering of Polymers. The effect of cross-linking density on sputtering is shown in Table IX for PVA hydrogels with two different cross-linking doses of 6.0 and 10.0 Mrads. The normalized change in N_{CO} was greatly decreased for the higher cross-linked sample. Analysis of

Table VIII
XPS Parameter Comparison of XPS Results of Swollen and Freeze-Dried P(VA-*co*-NVP) Copolymers with $F_1 = 0.59$

parameter	state	
	swollen	freeze-dried
I_C/I_O	1.56	1.36
I_N/I_O	0.17	0.24
I_C/I_N	8.96	5.26
γ_C, eV	2.4	2.5
γ_O, eV	1.9	2.5
γ_N, eV	1.7	1.7

Table IX
Effect of Sputtering on Freeze-Dried PVA and P(VA-*co*-NVP) Samples at Various Cross-Linking Densities

F_1	irradiation dose, Mrad	sputtering time, s	N_{CO}	N_{NO}	N_{CN}
1.0	6.0	0	2.03	0	
1.0	6.0	60	4.35	0.0	
1.0	6.0	120	6.26	0.0	
1.0	10.0	0	1.71	0.0	
1.0	10.0	120	2.13	0.0	
0.34	10.0	0	3.70	0.49	7.49
0.34	10.0	60	6.96	0.68	10.27

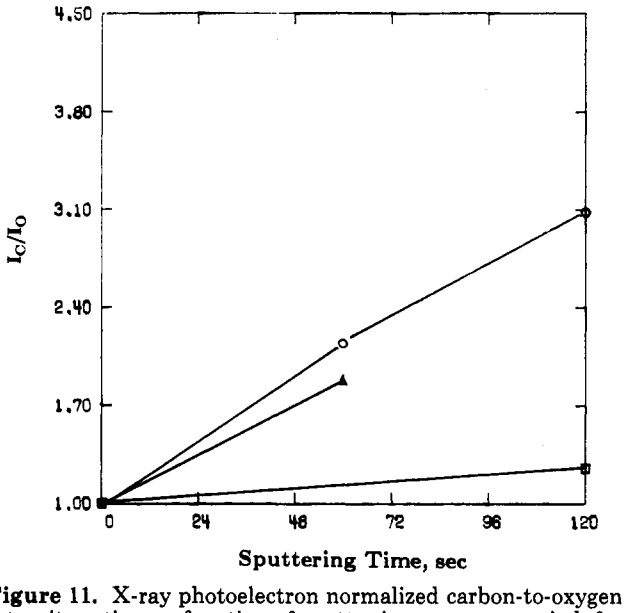

Figure 11. X-ray photoelectron normalized carbon-to-oxygen intensity ratio as a function of sputter ion exposure period, for a PVA hydrogel irradiated with 6 Mrad (○), a PVA hydrogel irradiated with 10 Mrad (□), and a P(VA-*co*-NVP) hydrogel ($F_1 = 0.34$) irradiated with 10 Mrad (△).

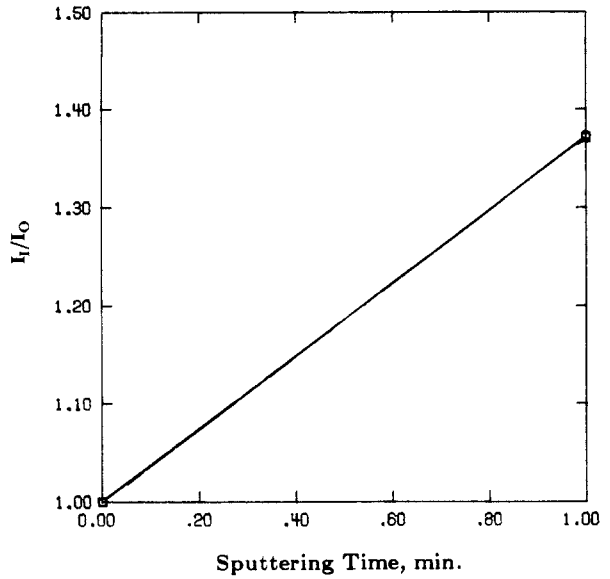

Figure 12. X-ray photoelectron normalized nitrogen-to-oxygen and carbon-to-nitrogen intensity ratios as a function of sputter ion exposure period.

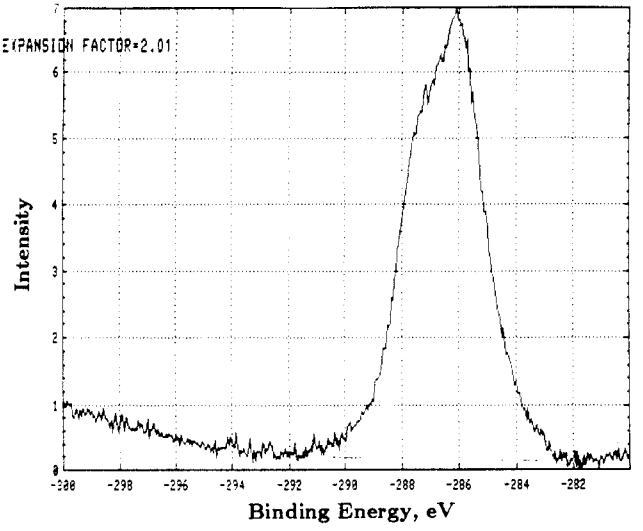

Figure 13. X-ray photoelectron C_{1s} spectrum of PVA (irradiated with 6 Mrad) before sputtering.

Table X
Photopeak Data For Native and Sputtered PVA Samples Produced by γ-Irradiation with 6 Mrad

sputtering time, min	position, eV		fwhm, eV		
	C_{1s}	O_{1s}	C_{1s}	O_{1s}	I_{CO}
0.0	286.0	533.6	3.1	2.1	0.82
3.0	284.7	533.0	2.4	2.4	2.32

Figures 11 and 12 demonstrated that the sputter yields of the elements of interest were $K_O > K_N > K_C$ or that the sputter yield increased.

Figures 13 and 14 show the C_{1s} spectra of a PVA hydrogel sample (F_1 = 1.0 and 6.0 Mrads) in the native state (before sputtering) and a PVA sample after 3 min of sputtering. Photopeak positions and values of fwhm for the native and sputtered PVA are presented in Table X. The carbon states of the sputtered sample approach pure aliphatic carbon. The reduction in carbon envelope fwhm was due to the removal of the PVA C–O states. The oxygen peak was essentially unchanged (differences in binding energy were probably due to charging effects) in the sputtered sample. Due to the low binding energy shifts

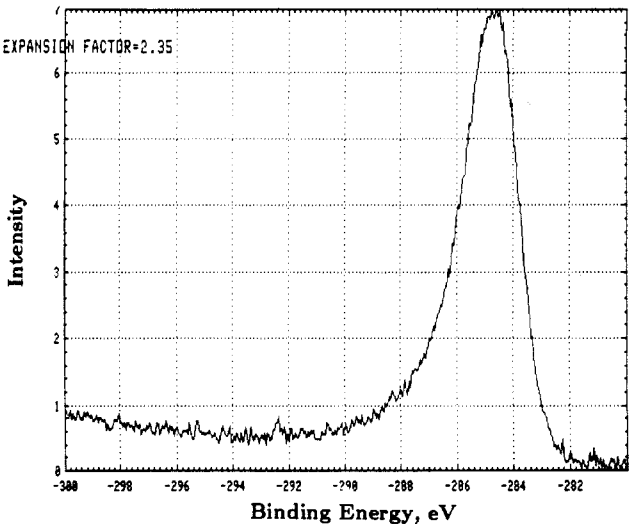

Figure 14. X-ray photoelectron C_{1s} spectrum of PVA (irradiated with 6 Mrad) after 3.0-min sputter period.

Table XI
XPS Results of Freeze-Dried PVA and P(VA-*co*-NVP) Samples Esterified with Heptafluorobutyric Acid

F_1	I_{CO}	I_{NO}	I_{FC}
0.13	1.86	0.39	0.05
0.17	1.69	0.44	0.23
0.34	1.46	0.31	0.50
1.00	0.84		0.86

of oxygen, multiple states of oxygen were not distinguished from the photopeak shape. The shift of surface-region carbon states toward aliphatic carbon with sputtering could have been the result of either thermodynamic factors or preferred sputtering. The polymer surface structure was obviously altered.

Surface Modification and Sputtering. To study the effect of freeze-drying on the surface-region composition, the surface hydroxyls of a series of copolymers were esterified by heptafluorobutyric acid chloride.

The selectivity of the esterification reactions was evaluated by labeling the PNVP homopolymer. XPS analysis of the PNVP sample demonstrated that fluorine was absent from the surface region of the sample. Thus the acyl chloride did not bind to the NVP structure.

The stability of the label to X-rays was evaluated by reexamination of an esterified P(VA-*co*-NVP) sample with F_1 = 0.34. Upon analysis of the C, O, N, and F 1s photopeaks a value of I_{FC} = 0.502 was obtained. The sample was reexamined without alterations and produced I_{FC} = 0.468. Thus, the label was unstable to X-rays, but the intensity reduction of the fluorine species was not severe.

The results of XPS analysis of several esterified hydrogels are presented in Table XI. The results showed that labeling occurred in the PVA and copolymer samples. With increasing VA content, the I_{FC} ratio increased and the I_{CO} ratio approached the PVA value. The I_{NO} ratio showed a maximum for the copolymer sample with F_1 = 0.17.

The C_{1s} photopeak of labeled PVA is presented in Figure 15. The peak located around 293 eV was the result of the CF_3 species of the label; the other C–F atoms produced the tailing of the peak to higher binding energies. The ratio of the intensity of the CF_3 peak to the total carbon intensity (including the CF_3 peak) was 0.02 (approximate due to the signal-to-noise ratio).

Quantitative analysis of the surface-esterified, freeze-dried hydrogels was attempted by assuming one label unit

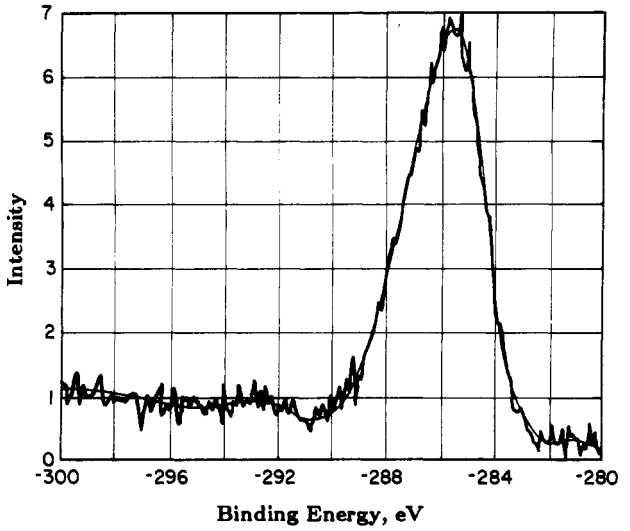

Figure 15. X-ray photoelectron C_{1s} spectrum of heptafluorobutyric acid chloride labeled PVA (irradiated with 2.28 Mrad).

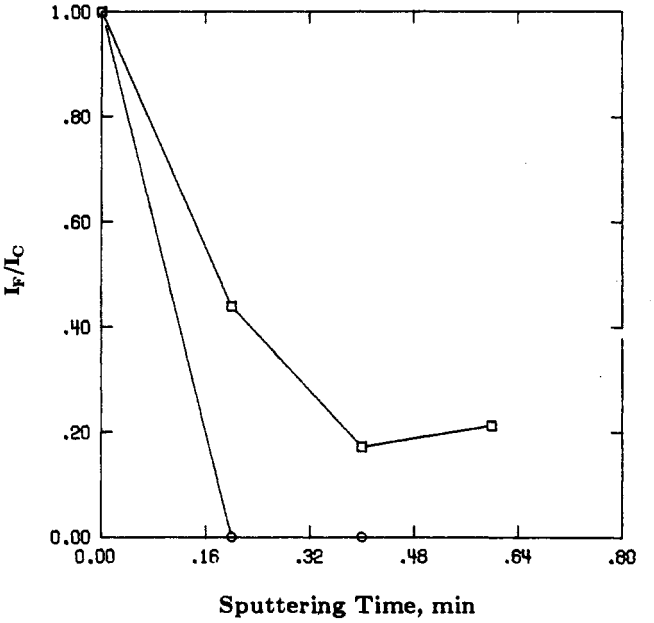

Figure 16. X-ray photoelectron fluorine-to-carbon intensity ratios as a function of sputter period for heptafluorobutyric acid chloride labeled P(VA-*co*-NVP) copolymers with $F_1 = 0.34$ (□) and $F_1 = 0.17$ (○).

per surface hydroxyl group. The results were inconsistent with bulk copolymer structure or unlabeled XPS results. For the amount of fluorine on the surface of the PVA sample, the carbon intensity was too high. This was probably due to surface contamination and variable labeling efficiencies. Further work will be required in this area.

Sputtering of Labeled Polymers. The labeled samples were sputtered and the depth of label penetration (as measured by the fluorine intensity) was estimated. All samples were cross-linked with irradiation of 2.28 Mrad. A plot of I_{FC} as a function of sputter time is presented in Figure 16 for the two copolymer samples. The I_{FC} ratio for the copolymer with $F_1 = 0.17$ dropped below measurable values very quickly. The I_{FC} ratio for the copolymer with $f_1 = 0.34$ dropped quickly but reached an asymptote after 24 s of sputtering. This could have been due to implantation of fluorine into the sample by the argon ions during sputtering. Analysis of the above sputter results (primary fluorine essentially removed by 24 s of sputtering) with sputter models indicated that the fluorine depth was approximately 200 Å. This would convert to a solid polymer depth of only 8 Å, indicating that the reaction was surface-specific and large-scale reorganization of the polymer surface with freeze-drying did not occur.

Conclusions

In conclusion, hydrogels of P(VA-*co*-NVP) copolymers of varying composition may be analyzed by X-ray photoelectron spectroscopy, upon freeze-drying. An enrichment of vinyl alcohol units on the surface of the copolymers was observed for $F_1 < 0.59$, when hydrogel surfaces prepared in contact with a glass surface were examined. These conclusions were substantiated by sputtering data obtained from the same samples.

Acknowledgment. The XPS studies reported here were performed at the University of Minnesota Regional NSF Instrumentation Facility (Grant No. CHE-79-16206). D.R.M. thanks the Amoco Foundation for a fellowship. Significant contributions by Prof W. N. Delgass are kindly acknowledged.

References and Notes

(1) Cooper, S. L.; Peppas, N. A.; Ratner, B. D.; Hoffman, A. S. *Biomaterials: Interfacial Phenomena and Applications*; American Chemical Society: Washington D.C., 1982; *Adv. Chem. Ser.* Vol. 199.
(2) Hench, L. L.; Ethridge, E. C. *Biomaterials: An Interfacial Approach*; Academic: New York, 1982.
(3) Salzman, E. W. *Interaction of the Blood with Natural and Artificial Surfaces*; Dekker: New York, 1981.
(4) Miller, D. R.; Peppas, N. A. *Biomaterials* **1986**, *7*, 329.
(5) Peppas, N. A.; Gehr, T. W. B. *J. Appl. Polym. Sci.* **1979**, *24*, 2105.
(6) Pennings, J. F.; Bosman, B. *Colloid Polym. Sci.* **1980**, *258*, 1099.
(7) Carlson, T. A. *Photoelectron and Auger Spectroscopy*; Plenum: New York, 1975.
(8) Miller, D. R.; Peppas, N. A. *J. Macromol. Sci., Rev. Macromol. Chem. Phys.* **1986**, *C26*, 33.
(9) Seah, M. P.; Dench, W. A. *Surf. Interface Anal.* **1979**, *1*, 2.
(10) Ratner, B. D. *Ann. Biomed. Eng.* **1983**, *11*, 313.
(11) Andrade, J. D. In *Surface and Interfacial Aspects of Biomedical Polymers*; Andrade, J. D., Ed.; Plenum: New York, 1985; p 105.
(12) Carley, A. F.; Joyner, R. W. *J. Electron Spectrosc. Relat. Phenom.* **1979**, *16*, 1.
(13) Kaelbe, D. H.; Moocanin, J. *Polymer* **1977**, *18*, 475.
(14) Gilding, D. K.; Paynter, R. W.; Castle, J. E. *Biomaterials* **1980**, *1*, 163.
(15) Hirokawa, K.; Danzaki, Y. *Surf. Interface Anal.* **1982**, *4*, 63.